China's urban EV ultra-fast charging distorts regulated price signals and elevates risk to grid stability

Qing Yu[1,4], Pengjun Zhao [1,2,4] ✉, Jiaxing Li[1,4], Han Wang[3], Jie Yan[3] & Haoran Zhang [1] ✉

The wide adoption of electric vehicles is driving the rapid deployment of ultra-fast charging stations, particularly in China. This study uses simulations based on extensive real-world charging data from major Chinese cities and finds that deploying 2000 ultra-fast charging stations in a city may increase the peak-to-valley differences of the public charging load by up to 31.61% daily relative to baseline cases. While integrating energy storage systems can help smooth short-term load volatility, it may simultaneously exacerbate short-term demand surges, particularly during the transition from high- to low-price periods. Under an unregulated scenario, large-scale deployment of ultra-fast charging stations with energy storage could raise peak loads by over 70–85% by 2030 and multiply them by up to 7.5 times by 2050. These findings underscore that a comprehensive rethinking of grid management strategies and market frameworks will be essential to ensure urban energy resilience in an era of rapid electric vehicle expansion.

The Paris Agreement has galvanized global efforts to limit the average global temperature increase to well below 2℃ above pre-industrial levels[1]. The shift towards electric vehicles (EVs) is crucial in this effort, recognized universally as key for reducing greenhouse gas emissions[2,3]. As the number of EVs grows, there is a growing demand for adequate and efficient charging infrastructure. The construction of Ultra-fast Charging Stations (UFCS) is particularly important, as they promise to significantly slash charging times and boost user convenience by allowing EV charging in 5–10 min[4–8]. The capability of fast charging, supported by high-voltage technologies, is seen as a necessary advancement to keep pace with the growing fleets of EVs[9]. In China, the government has set explicit targets to deploy 360,000 high-power charging stations (≥350 kW) by 2025 under the National New Infrastructure Plan, with fiscal subsidies covering 30% of equipment costs[8,10]. This aligns with the national goal to achieve 80% EV penetration in public transport by 2030[11]. Pilot cities like Shenzhen and Shanghai are mandated to install ultra-fast chargers in over 90% of

highway service zones by 2024, ensuring 5 min charging accessibility for 80% of urban EV owners[12].

Managing the escalating electricity demand driven by the swift uptake of EVs is a global challenge. A critical policy tool implemented worldwide is the Time-of-Use (TOU) pricing system, adopted in countries including the United States, Canada, Spain, and China[13–16]. TOU pricing strategically adjusts electricity rates over the course of the day to mirror fluctuations in demand, thereby creating regulated price signals that prompt consumers to modify their electricity consumption patterns[17,18]. During peak demand periods, when the electrical grid faces maximum stress, prices rise sharply. Conversely, rates decrease during off-peak hours, providing economic incentives for consumers to reschedule energy-intensive activities, such as the charging of EVs, to these less burdensome times[19–21].

However, recent empirical studies have raised significant concerns regarding TOU pricing, particularly its unintended consequence of inducing sharp spikes in charging demand immediately at the

[1]School of Urban Planning and Design, Peking University Shenzhen Graduate School, Shenzhen, Guangdong, China. [2]School of Urban and Environmental Science, Peking University, Beijing, China. [3]State Key Lab of Alternate Electrical Power System with Renewable Energy Sources, School of New Energy, North China Electric Power University, Beijing 102206, China. [4]These authors contributed equally: Qing Yu, Pengjun Zhao, Jiaxing Li. ✉e-mail: pengjun.zhao@pku.edu.cn; h.zhang@pku.edu.cn

beginning of lower rate periods, a trend exacerbated by the widespread adoption of UFCS[22,23]. This clustering of demand not only undermines the intended benefits of TOU pricing-aimed at smoothing electricity consumption-but also heightens grid strain, potentially reversing its utility in enhancing grid stability[24–28]. The crux of the issue lies in the misalignment between swiftly advancing charging technologies and the more gradually evolving electricity market frameworks, which continue to operate under outdated energy paradigms[29–31]. This misalignment distorts critical regulated price signals meant to balance electricity supply and demand, leading to grid inefficiencies and instability[32–34].

In this work, we conduct a data-driven simulation of ultra-fast charging station roll-out across Beijing, Shanghai, and Guangzhou, leveraging over 760,000 real-world public charging records. Our results show that large-scale deployment of these chargers increases the peak-to-valley differences of the total public charging load, substantially stressing grid flexibility and adequacy margins. We also find that while integrating on-site energy storage can smooth short-term load volatility, it can simultaneously exacerbate demand surges during electricity price changes. The analysis underscores that without new controls, deploying fast chargers with energy storage can significantly raise peak loads, highlighting the need for strategies to unlock their grid-stabilizing potential.

Results

Simulating deep UFCS adoption

According to China's New Energy Vehicle Industrial Development Plan for 2021 to 2035, by 2030 and 2060, the penetration rate of NEVs, primarily EVs, in vehicle ownership needs to reach 20% and 100%, respectively[35]. To meet the rapidly growing demand for EV charging, the deployment of UFCS is essential. Our analysis focuses specifically on the charging demand of light-duty (LD) passenger vehicles, as they constitute the predominant user base for public urban charging infrastructure, including the UFCS central to our study.

The planning of UFCS in major Chinese cities reveals ambitious targets. For instance, Shenzhen aims to construct 300 UFCSs by 2025, increasing to 1,000 by 2030. Similarly, Beijing plans to establish 500 UFCSs by 2024 and reach 1,000 by 2025. Each station is typically equipped with 1 or 2 ultra-fast chargers with power outputs above 480 kW, along with 2 to 7 fast chargers with power outputs exceeding 250 kW. While current LDVs typically support DC fast charging rates between 60 and 250 kW, the deployment of 480 kW+ UFCS anticipates future advancements in vehicle battery technology, enabling charging times of 5−10 min. Under this trend, it is estimated that high-power chargers (240 kW+) could make up 44% of public chargers by 2030 and 80% by 2035[36].

Figure 1a illustrates a data-driven framework to simulate and model the dynamic fluctuations in EV charging load under UFCS deployment, assessing the impact of UFCS expansion on grid load (Fig. 1b shows the principle of how UFCS affects grid load). This study focuses on three major cities: Beijing, Shanghai, and Guangzhou. The basic characteristics of these cities and the TOU policy are summarized in Table 1. Although each city has implemented a TOU strategy, the actual charging prices at different stations may still vary; the distribution is provided in Supplementary Note 1. It is important to note that electricity tariffs for commercial and industrial users in China typically follow a two-part system, comprising an Energy Charge (often structured as TOU pricing, as detailed in Table 1) based on energy consumption, and a Capacity Charge based on peak power demand. However, under current supportive policies aimed at promoting EV infrastructure development, public centralized EV charging and swapping stations in cities like Beijing, Shanghai, and Guangzhou are temporarily exempted from the Capacity Charge.

The methodology first involves categorizing the charging stations and assuming that commercial and workplace stations will gradually be upgraded to UFCS. Three simulation scenarios were defined for the years 2030, 2035, and 2050. For each simulation scenario, a specified number of these stations are modeled as upgraded, and the upgraded
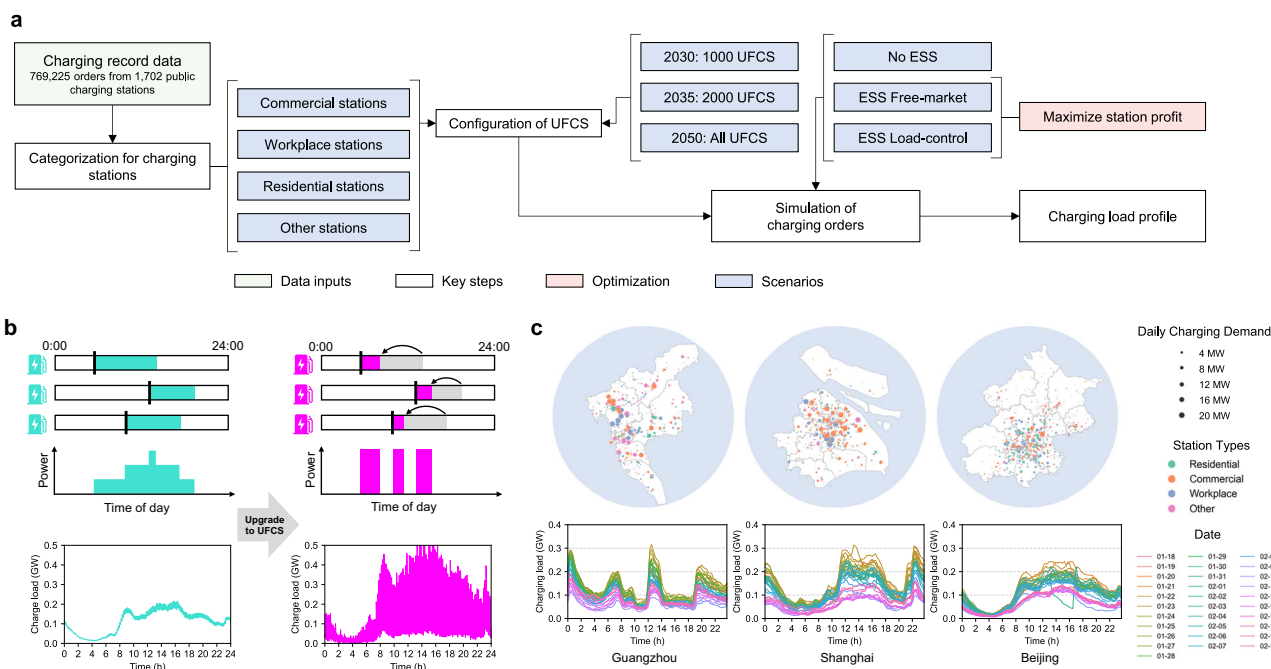

Fig. 1 | Modeling Framework for Urban Charging Load under Ultra-fast Fast Charging System (UFCS) adoption. a shows an overview of the modeling approach, where charging record data serves as the input, the model categorize charging stations and configures UFCS in multiple scenarios and introduces an optimization model to simulate on-site Energy Storage System (ESS) deployment under unregulated market and load-control scenarios, ultimately deriving the charging load profile under UFCS adoption. **b** illustrates the concept of simulating UFCS by upgrading existing charging stations to UFCS, thereby shortening charging durations and potentially increasing fluctuations in the city's total charging load. **c** presents charging record data from 1,702 charging stations across Guangzhou, Shanghai, and Beijing with various land use types, used to estimate the charging load profiles of the three cities.

Table 1 | Basic characteristics and Electric Vehicle (EV) infrastructure in three major Chinese cities (2023)

Category		Beijing	Guangzhou	Shanghai
Population (× 10⁴)		2,185.8	1,887.3	2,484.6
Average Income($/month)		1,641	1,841	1,717
Number of EVs (× 10³)[69–71]		773	843	1,288
Number of Public Chargers (× 10³)[72]		129	53	79
Public Charging Stations (× 10³)		8.09	3.08	8.66
TOU Pricing Schedule[73–75]	Low price (Valley hours)	23:00-7:00	0:00-8:00	22:00-6:00
	Medium price (Off-peak hours)	7:00-10:00 13:00-17:00 22:00-23:00	8:00-10:00 12:00-14:00 19:00-24:00	6:00-8:00 11:00-18:00 21:00-22:00
	High price (Peak hours)	10:00-13:00 17:00-22:00	10:00-12:00 14:00-19:00	8:00-11:00 18:00-21:00

UFCS are integrated with the non-upgraded stations to simulate the overall grid load. Additionally, we introduced an optimization model to simulate the deployment of on-site ESS, with unregulated market and load-control scenarios. The simulation results provide detailed spatiotemporal profiles of charging loads with minute-by-minute resolution, offering insights into the interplay between UFCS deployment and grid dynamics.

In detail, charging order data from public charging stations serves as the primary input for the study. The dataset includes 1,702 charging stations (representing ~8.6% of the estimated 19,830 total public stations across the three cities, see Table 1) and a total of 769,225 charging orders recorded over a 31 day period (from January 18 to February 17, 2024) across the three cities. Figure 1c shows the load of different types of charging stations in the three cities and the total charging load at the city level. Analysis of this 2024 data reveals that ultra fast chargers meeting the 480 kW specification were virtually absent in our sample (only one such charger was present across the three cities, with 94.8% of chargers being 120 kW or less). Given this observation, we consider the current charging landscape represented by the 2024 dataset to be effectively free of the widespread adoption of next generation 480 kW UFCS, and it is therefore utilized as the baseline (pre-UFCS adoption in 2024) for our study. These data reflect real-world charging demand, exhibiting distinct temporal patterns influenced by factors such as TOU pricing schedules (detailed analysis in Supplementary Note 2). These samples are representative of high quality, as they were sourced from a single major charging station platform rather than from different platforms. Assuming that the dataset represents a uniform sampling of public charging stations, we scaled the data to align with the actual distribution of charging stations within each city to represent the citywide charging load of public charging stations. This scaling process preserves the aggregated charging patterns observed in our sample, which reflect user behaviors under the current TOU schedules and the existing station-specific price variations. Our simulation then focuses on the impact of upgrading charging speeds on the power load under these established demand patterns.

Considering the constraints of urban land use, deploying a large number of completely new UFCS sites is challenging. Therefore, our UFCS adoption assumption for future scenarios involves upgrading existing charging infrastructure rather than building entirely new stations. Given the varying demand characteristics by location and land use, the choice of upgraded points significantly impacts the resulting load profile. For example, daytime charging demand tends to concentrate in employment centers, whereas residential areas typically see higher evening demand. For the UFCS simulation, we first categorized the existing charging stations into "Residential," "Commercial," "Workplace," and "Other" based on station address and name information (see Methods section for classification details; the load profile of different types of stations is provided in Supplementary Note 4). As fast charging stations are generally more often located in commercial districts and workplaces to maximize revenue, these

categories were prioritized as candidate sites for upgrading to 480 kW UFCS in the initial scenarios.

Three scenarios were established based on city targets: deploying 1000 UFCSs by 2030, 2,000 by 2035, and replacing all public charging stations with UFCSs by 2050. In the 2030 and 2035 scenarios, commercial and workplace charging stations were prioritized for upgrade, whereas the 2050 target encompasses the conversion of all public charging stations to UFCS, with each UFCS configured with two 480 kW ultra-fast chargers. To reduce random errors, we performed multiple sampling tests for each scenario to reflect overall trends.

UFCS distortion of TOU-based regulated price signals

TOU tariffs have emerged as a particularly effective tool, clearly influencing when and how EV owners choose to charge their vehicles. The effectiveness of TOU in shifting load is substantiated by comparing observed charging patterns with a simulated baseline scenario without TOU influence (see Supplementary Note 3 for details on the Shanghai case study), based on the method proposed in our previous study[37]. This comparison reveals that without TOU, charging demand would likely peak during post-commute hours, whereas the actual data shows a significant shift towards off-peak and valley price periods. Our analysis of EV charging patterns across Guangzhou, Beijing, and Shanghai illustrates the significant impact of TOU tariffs (as is shown in Fig. 2). These tariffs, which offer lower rates during off-peak hours, have successfully shifted the bulk of EV charging to nighttime, reducing the strain on the urban power supply during high-demand periods. This shift is evident across all three cities, regardless of local differences in the specific timing of these tariffs. For instance, in Guangzhou, the valley hours with low electricity price period extend from midnight to 8:00 AM, during which there is a noticeable increase in charging activity shortly after midnight and again just before the period ends. Although Beijing and Shanghai have earlier end times for their off-peak periods, the pattern of increased charging activity during these hours remains consistent. This demonstrates a widespread behavioral adaptation among EV owners, who are keen to take advantage of lower electricity prices, thereby underscoring the clear effectiveness of TOU tariffs in managing energy consumption patterns in urban China.

While the TOU tariffs have been successful in redistributing load times, the integration of UFCS presents a challenge to this established pattern. UFCS allow for quicker battery replenishment, which, while convenient, leads to intense, short-term demand spikes. These load peaks are particularly acute during the shift from peak to off-peak tariffs, as many users wait to plug in their vehicles until the lower rates take effect. Such synchronization of charging behavior results in a dramatic increase in electricity demand exactly at the onset of the off-peak period. The magnitude of these spikes is further exacerbated by the rapid charging capabilities of UFCS, which, if adopted at a large scale, could see peak load demands doubling compared to non-UFCS scenarios.
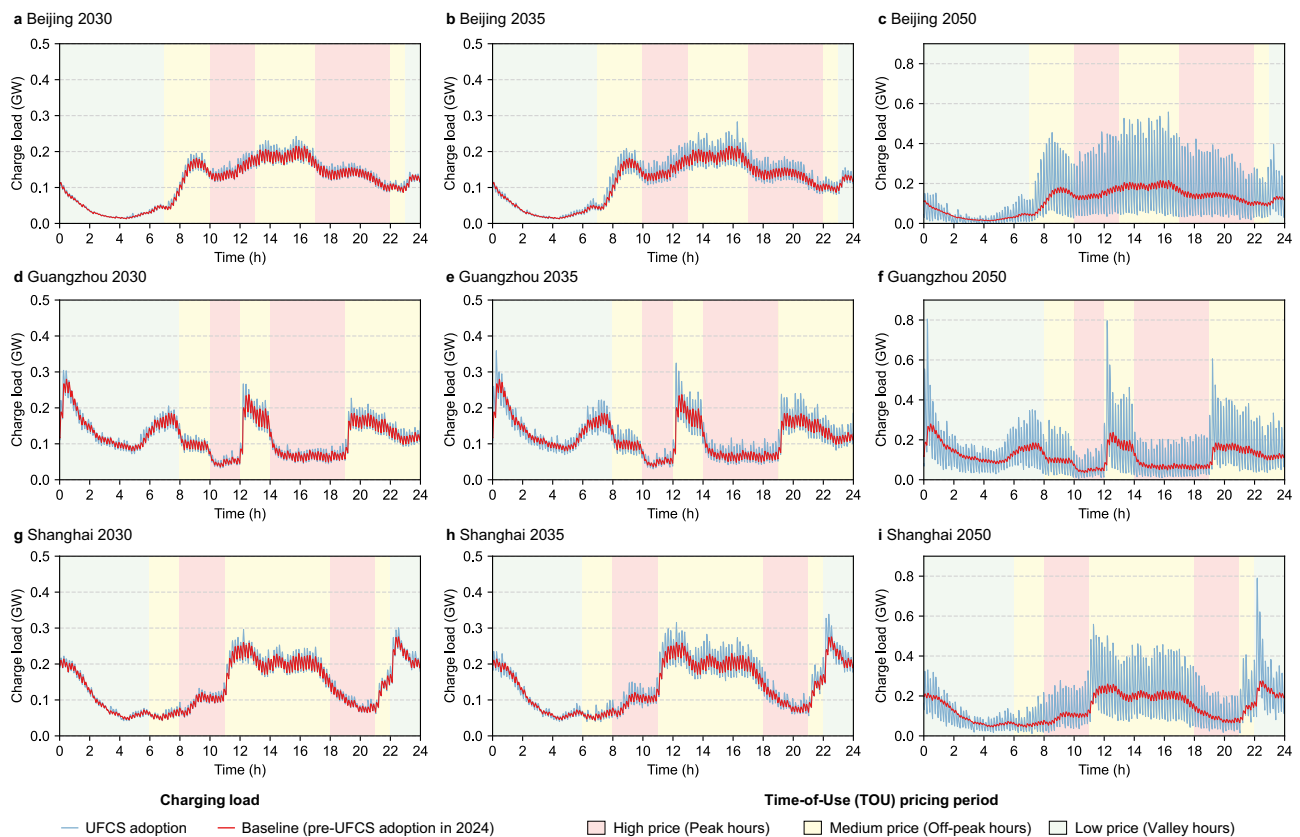
Fig. 2 | Daily charging load profiles across the three cities before and after Ultra-fast Fast Charging System (UFCS) deployment under the 2030, 2035, and 2050 scenarios. Our model simulates the charging load under UFCS deployment based on real charging orders and compares it with the current scenario. **a–g** show the load profiles for Beijing, Guangzhou, and Shanghai, respectively, under the deployment of 1,000 UFCS in 2030. **b–h** represent the load profiles for the deployment of 2,000 UFCS in 2035, while (**c–i**) illustrate the charging load profiles for the scenario in 2050, where all public charging stations are converted to UFCS.

The introduction of UFCS is anticipated to significantly amplify the variability of charging loads, leading to a pronounced increase in the short-term peak-to-valley load differences in the power grid. High peak-to-valley differences require the grid to adjust power output frequently to accommodate short-term fluctuations, which may induce instability in grid frequency and voltage, increasing the risk of grid faults and raising operational and maintenance costs. This instability ultimately threatens the reliability and stability of the power supply. To quantify these fluctuations, we use two key metrics: the daily peak-to-valley difference (the difference between the maximum and minimum load observed over a 24-hour period, representing the overall daily load swing) and the maximum hourly peak-to-valley difference (the maximum difference between the peak and valley load observed within any one-hour window during the day, quantifying short-term load volatility). Using simulation results, we calculated these differences in charging demand under various UFCS deployment scales and compared them with baseline EV public charging load levels (pre-UFCS adoption in 2024), as illustrated in Fig. 3.

As illustrated in Fig. 3a,b, expanding the UFCS network increases the daily peak-to-valley load gap almost linearly in all three cities. Up to roughly 1,500 stations, the trend is similar, but beyond that point, Guangzhou's curve rises much faster than Shanghai's, which in turn exceeds Beijing's. This is attributable to the inherently higher baseline volatility of its charging load, driven by Guangzhou's more frequently adjusted daytime TOU price periods.

From the daily peak-to-valley difference perspective (Fig. 3a), by 2030, deploying 1,000 UFCS is projected to increase the total public charging load peak-to-valley difference by up to 13.70% on a daily average basis and by 19.72% for short-term hourly differences compared to the non-UFCS baseline. By 2035, deploying 2,000 UFCS may elevate these differences by up to 31.61% (daily) and 46.15% (short-term). When the number of stations reaches 3,000, the increase in peak-to-valley difference is expected to reach 49.22% (daily) and 75.12% (short-term). Furthermore, due to the inherently higher volatility of charging load under the existing TOU policy in Guangzhou compared to other cities, the risks associated with UFCS deployment are significantly greater for Guangzhou than for the other two cities.

As illustrated in our simulation, once a valley pricing period begins, UFCS operators and EV users converge in their charging activities, triggering "secondary peaks" or even new "late-night peaks." This pattern of demand reveals a critical mismatch between the fast-paced adoption of high-power ultra-fast charging technologies and the existing electrical grid and market designs, which still largely cater to traditional, steadier consumption patterns. The current market mechanisms, which prioritize short-term economic gains, fail to align with the long-term sustainability goals of environmental policies promoting EVs and renewable energy sources. This discord not only increases the risk of grid overload but also hinders investment in renewable energy, as the market fails to provide stable and favorable signals for such investments due to the intermittent nature of renewables juxtaposed against the peak demands of UFCS.

Grid risks amplified by UFCS under TOU pricing

The widespread deployment of UFCS under current TOU tariffs is expected to significantly increase peak charging power demand and short-term load volatility, introducing potential risks to power grid stability and adequacy. These risks primarily manifest as potentially
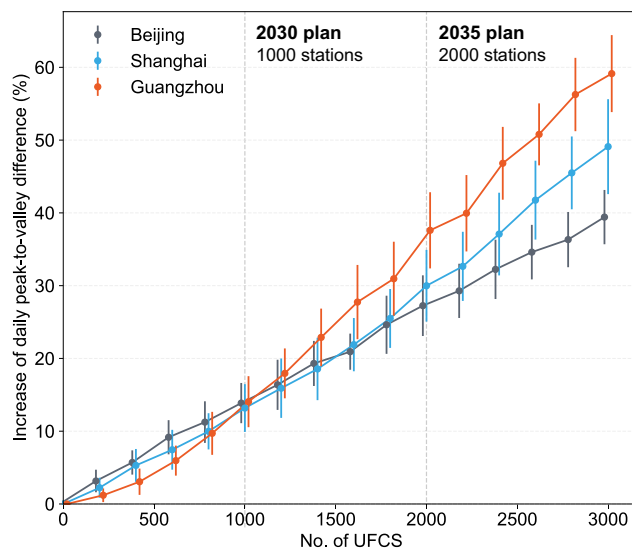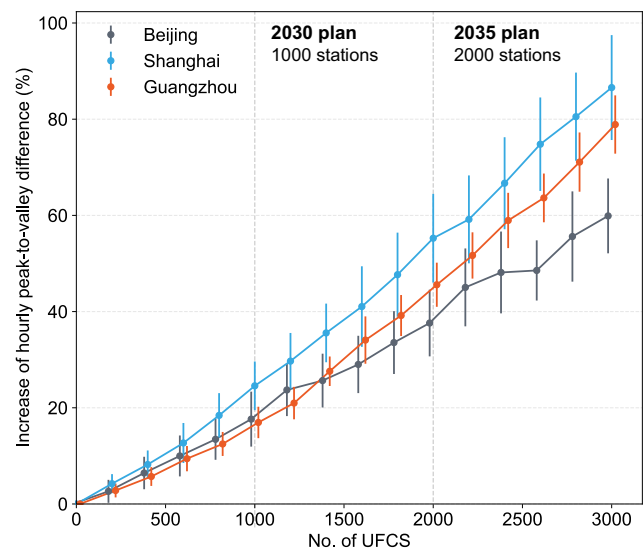
a Daily peak-to-valley

b hourly peak-to-valley

Fig. 3 | Impact of Ultra-fast Fast Charging System (UFCS) deployment on Electric Vehicle (EV) charging load peak-to-valley difference. a shows the percentage increase of the daily peak-to-valley difference, indicating the total range of load variation encountered by the grid on a full 24-hour period; while (**b**) displays the percentage increase of the maximum hourly peak-to-valley difference, indicating the most significant load swing that occurs within any single hour, reflecting the potential for rapid demand changes that are characteristic of high-power charging events. Points and the error bars on the lines indicate the mean value and standard deviation derived from $M = 50$ independent simulations for each deployment scale (at intervals of 250 UFCS).

exceeding the grid's flexibility resources (Regulating Reserves) and its allocated power capacity (Capacity Reserves).

Power systems maintain stability and adequacy through various ancillary services, including Regulating Reserve (RR) and Capacity Reserve (CR)[38,39]. RR provides rapid-response capabilities in seconds to minutes to continuously balance supply and demand, managing fluctuations and maintaining system frequency; it addresses the grid's need for flexibility against rapid load ramps. CR represents available capacity generation or demand-side resources held in reserve to ensure the system can meet peak load and handle contingencies; it addresses the grid's need for adequacy to meet the magnitude of demand. The unique characteristics of UFCS-high power and potential for synchronized charging-can significantly increase the demand for both RR and CR compared to baseline conditions. It is important to recognize that while RR and CR are typically planned and dispatched by the grid operator across broader regional control areas (e.g., provincial level), the significant new stress and demand for these reserves originates from concentrated load centers. Large-scale UFCS deployment is primarily an urban phenomenon, and our simulations appropriately focus on quantifying the impact and the resultant demand for reserves generated at the city level.

A significant risk associated with UFCS deployment is the possibility of depleting the system's RR - the fast-responding flexibility margin (AGC units, BESS, responsive load) that grid operators rely on to correct second-to-minute imbalances and keep frequency within tight bounds. Risk occurs when rapid or sudden variations in charging demand exceed the grid's capacity to regulate and maintain stable operation via available RR, potentially leading to frequency instability or voltage fluctuations. Our simulations show that UFCS demand spikes-especially those clustered immediately after morning and evening TOU price transitions-can momentarily push the incremental balancing requirement above the available RR, creating a non-negligible probability of frequency or voltage excursions. Figure 4a–f plots, for Beijing, Guangzhou, and Shanghai in 2030 and 2035, the time-of-day profile of the probability of exceeding three illustrative RR thresholds, highlighting the intervals of greatest operational stress.

Furthermore, the high-power nature of UFCS places substantial short-term stress on local grid capacity, creating a risk of exceeding the CR. We define the baseline as the maximum simulated public-charging load in a non-UFCS scenario and impose three illustrative reserve buffers-15%, 20%, and 25%-in line with leading planning-reserve guidelines, which all recommend maintaining total reserve margins in the 15–20% range of system peak load[38,40,41]. Applying these percentages specifically to the public-charging component allows us to isolate the incremental capacity stress introduced by UFCS. Figure 4g–i plots, for each city, the probability that the aggregate charging load surpasses the three CR thresholds as UFCS deployment scales up. The results reveal that 15% CR becomes insufficient once 1,000 UFCS are deployed in the 2030 case, as all three cities register a non-negligible chance of reserve exhaustion. 25% CR remains adequate only up to 1,500 UFCS, as beyond that level, approaching the 2035 target of 2,000 stations, the exceedance probability again rises sharply. Consequently, adherence to the current Chinese planning standard of 20% total reserve would leave the grid increasingly exposed between the 1,000 station and 2,000 station milestones, signaling that capacity-reinforcement or alternative flexibility measures will become imperative in the 2030–2035 window.

These results demonstrate that the large-scale integration of UFCS under the current TOU pricing model significantly increases grid risks, specifically the risk of exceeding RR due to heightened volatility and the risk of exceeding CR due to elevated peak public charging demand. This heightened risk arises from pronounced demand spikes during periods of lower tariffs, leading to potential challenges in managing rapid load variations and ensuring sufficient capacity. These issues necessitate urgent and comprehensive enhancements to grid management strategies, including the potential expansion of CR allocated for charging infrastructure and improvements in grid flexibility, potentially supported by enhanced RR or sophisticated demand response programs. Adapting these strategies is essential to effectively manage the substantial changes in energy consumption patterns and maintain the reliability and efficiency of the electrical grid as UFCS becomes more prevalent.
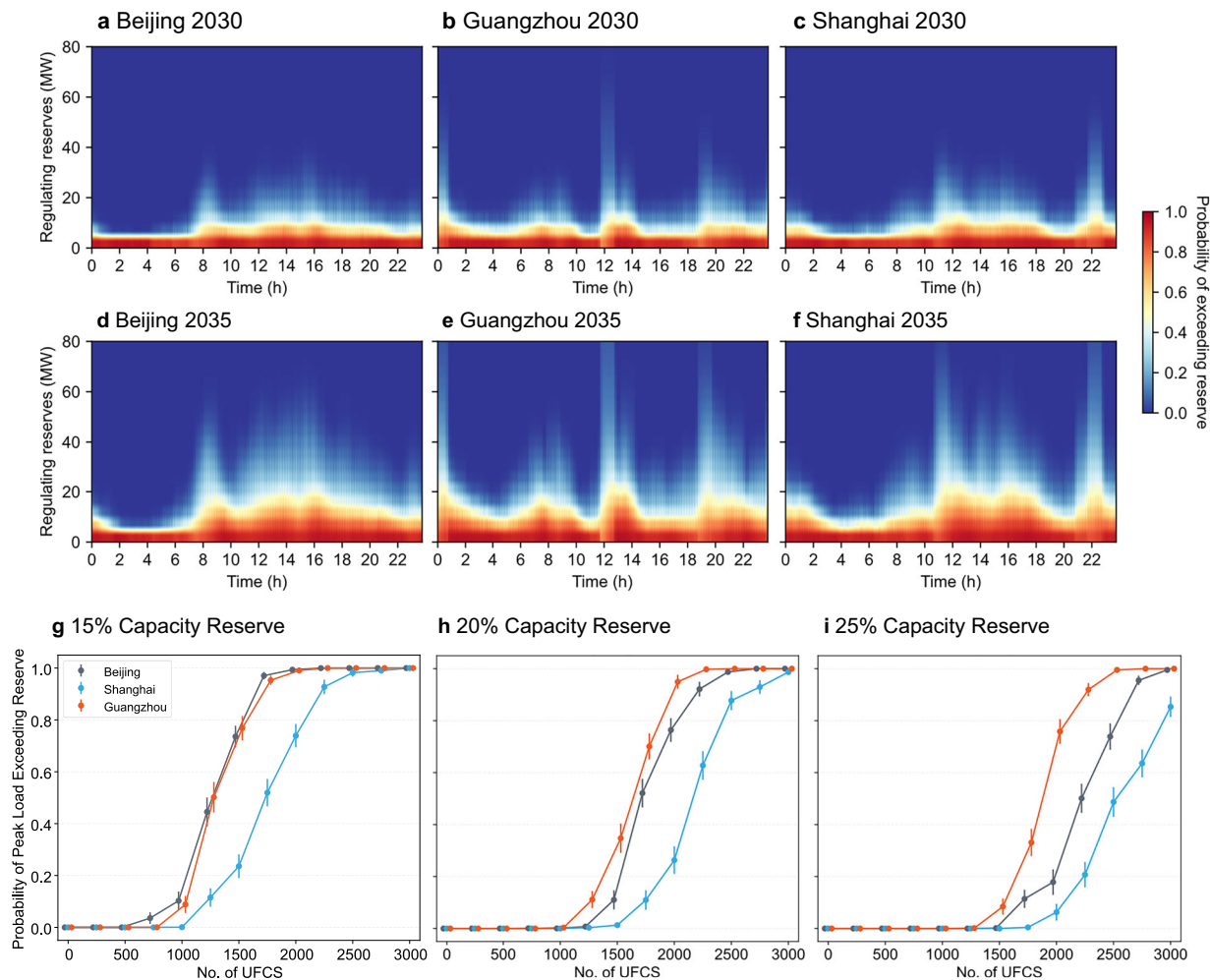
Fig. 4 | Grid stability risks induced by Ultra-fast Fast Charging System (UFCS) deployment. a–f Temporal distribution of the probability of exceeding illustrative Regulating Reserve levels in Beijing (**a, d**), Guangzhou (**b, e**), and Shanghai (**c, f**) for 2030 (**a–c**) and 2035 (**d–f**). **g–i** probability of exceeding Capacity Reserve thresholds under different UFCS deployment scales. The thresholds represent the baseline maximum charging load plus an additional reserve margin equivalent to 15% (**g**), 20% (**h**), or 25% (**i**) of the maximum simulated charging load. Points and the error bars on the lines indicate the mean value and standard deviation derived from $M = 50$ independent simulations for each deployment scale (at intervals of 250 UFCS).

Risk of grid instability from improper ESS management in UFCS

The integration of ESS with UFCS primarily aims to enhance profitability through energy arbitrage-buying energy at lower prices during off-peak hours and selling during peak prices. However, while this approach can significantly enhance the economic returns of charging station operations, it also introduces new challenges in terms of grid stability. The use of ESS allows charging stations to disconnect from grid electricity prices temporarily, charging their batteries when it is cheapest and discharging during periods of highest electricity prices. This behavior can lead to increased load fluctuations as stations switch between drawing power from the grid and supplying power from their storage systems.

To evaluate the operational dynamics of UFCS equipped with on-site ESS, we developed a model to simulate operation strategies of ESS-integrated UFCS. This simulation investigates how on-site ESS impacts the total charging load under various market conditions. We focus on three key scenarios:

The first is an Unregulated Market Scenario, where stations operate solely based on market dynamics to maximize cost savings. The second is a Capacity Charge Scenario, in which the standard TOU tariff is augmented with a capacity charge to incentivize stations to shave peak load. The third is a Demand Response Scenario, where grid operators implement direct control measures to ensure grid stability.

Figure 5 presents the simulation results across three cities for future scenarios under the following configurations: UFCS without ESS, UFCS with ESS under different scenarios. Generally, ESS integration significantly reduces daytime power demand and fluctuations compared to the UFCS-only case, leading to smoother daytime load curves (Fig. 5a–i) and enhanced grid stability during peak hours.

However, the Unregulated Market scenario reveals a critical risk: a substantial increase in nighttime demand and volatility. As shown in Fig. 5a–i, the transition from peak/shoulder to off-peak pricing under the TOU tariff (around hour 23 in Beijing, hour 22 in Shanghai, and hour 0 in Guangzhou) triggers a synchronized surge in charging activities as stations replenish their ESS during newly available low-price periods. Without regulatory constraints, ESS exacerbates this issue, concentrating energy demand. This potential grid risk is quantified in Fig. 5j,k. Deploying 1,000 UFCS stations with ESS under this scenario significantly increases peak demand: in 2030, the peak load rises by 71.4% in Beijing (0.239 GW to 0.410 GW), 84.6% in Guangzhou (0.308 GW to 0.569 GW), and 83.5% in Shanghai (0.306 GW to 0.562 GW) compared to the baseline without ESS. By 2050, under full deployment, these unregulated peaks could reach 4.31 GW, 3.17 GW, and 3.67 GW respectively, approximately 7.5, 3.9, and 4.6 times higher than without ESS. The average hourly peak-to-valley difference also increases compared to the UFCS-only case (Fig. 5k).
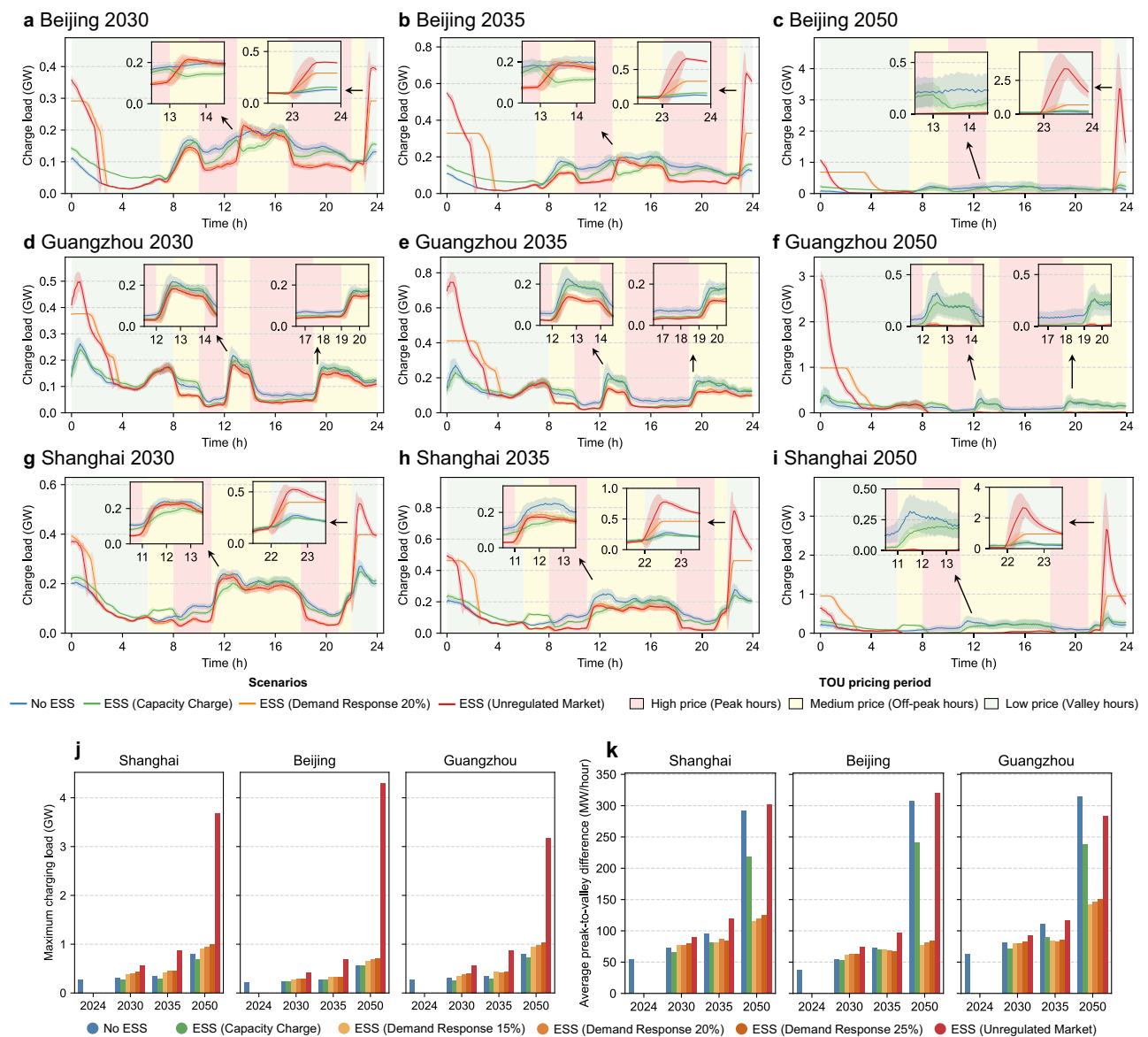
Fig. 5 | Impact of on-site Energy Storage System (ESS) integrated Ultra-fast Fast Charging System (UFCS) on charging load. a–i depict the charging load profiles under different scenarios: no ESS, ESS with capacity charge scheme, ESS with demand response control (under 20% of CR), and ESS in an unregulated market scenario, across 2030, 2035, and 2050 deployment timelines in three cities. Shaded areas represent the mean ± standard deviation over a 30 min window started at each time point. (**j**, **k**) illustrate key metrics for assessing charging load stability in these scenarios, with (**j**) showing the maximum charging load and (**k**) presenting the average hourly peak-to-valley difference.

This nighttime surge presents a dual nature. On the negative side, the onset of the low-price period under the TOU tariff overlaps with the residual nighttime load peaks, thereby exacerbating the risk of grid overloading. On the positive side, the relatively extended duration of the low-price window provides operational flexibility, enabling the deferral of charging activities without compromising energy replenishment objectives. Given these conditions, the implementation of control strategies during this period is both necessary and practically achievable.

In contrast, both the Capacity Charge and Demand Response scenarios effectively mitigate these nighttime surges and improve overall load profiles (Fig. 5a-i). Comparative analysis using key metrics (Fig. 5j,k) highlights their distinct mechanisms and trade-offs. The Capacity Charge scenario, by introducing a financial penalty for high peak demand, incentivizes users to autonomously adjust ESS operations. This leads to constructive grid behavior, suppressing peak loads

and mitigating fluctuations without direct intervention. It aligns individual economic optimization with grid stability objectives.

However, under the fully deployed ESS scenario in 2050, the Capacity Charge strategy faces limitations. To avoid creating new, penalized nighttime peaks, stations might limit their nighttime charging, potentially underutilizing ESS capacity and reducing its effectiveness in smoothing daytime load. Conversely, Demand Response scenarios, through direct control, can ensure ESS is fully charged during off-peak periods without creating uncontrolled peaks. This allows ESS to more effectively minimize reliance on grid energy during daytime operations and maximize its contribution to mitigating daytime grid stress.

These findings highlight that both pricing-based (Capacity Charge) and control-based (Demand Response) strategies possess distinct advantages and limitations. Careful and coordinated design of incentive and management mechanisms will be essential to fully

harness the potential of ESS in stabilizing future power systems under deep UFCS deployment.

Discussion

As China accelerates its transition to an electrified transportation system, the proliferation of EVs supported by UFCS technology marks a critical advancement[42]. UFCS dramatically shortens charging times, enhancing convenience and promoting EV adoption (an initial assessment of potential socioeconomic benefits of UFCS is provided in Supplementary Note 5). However, this technological leap creates a fundamental tension with China's existing TOU pricing mechanisms. While TOU tariffs are designed to incentivize off-peak electricity consumption, they inadvertently encourage a synchronized rush to charge when prices are lowest, as highlighted by related studies[23,43].

Building on these empirical observations, our study developed a simulation model based on real-world public charging records to simulate a large-scale UFCS rollout across three major Chinese cities. Our findings provide quantitative evidence that this combination results in exceptionally sharp, high-magnitude demand spikes. The consequent high ramp rates strain grid infrastructure and necessitate increased fast-responding reserves, confirming a significant threat to grid flexibility and adequacy margins[44,45].

Furthermore, our analysis of on-site ESS reveals a critical duality. While much of the literature has focused on the economic benefits and profit-maximization strategies for ESS operators through arbitrage[46,47], our results expose a significant potential negative externality. Unregulated, arbitrage-driven ESS operation, while profitable for the station, can create new and even more severe demand peaks during low-price periods. This finding suggests that realizing the grid-stabilizing potential of ESS is not automatic and requires integrated policy frameworks.

The grid instability induced by UFCS fundamentally undermines the effectiveness of the current TOU model and complicates broader energy policy goals. The sharp, unpredictable demand patterns make it significantly more difficult to integrate intermittent renewable energy sources like wind and solar, which rely on a stable and predictable grid[48,49]. This misalignment also challenges the economic rationale behind China's substantial investments in grid modernization and renewable capacity[50,51]. By eroding demand predictability, the unregulated rollout of UFCS jeopardizes the financial models that underpin these critical long-term investments, potentially impeding progress towards China's decarbonization targets.

In conclusion, while UFCS technology is a catalyst for sustainable transportation in China, its integration exposes critical vulnerabilities in the existing electricity market structure. Our findings reveal that the combination of UFCS and conventional TOU pricing can severely compromise grid stability, a problem potentially exacerbated by arbitrage-driven energy storage systems. Therefore, realizing the full benefits of electrified transport requires a strategic evolution of policy and infrastructure. This necessitates moving beyond static TOU tariffs towards more dynamic pricing models that can adapt to real-time grid conditions. Critically, integrated policy frameworks must be developed to govern ESS operation, ensuring they function as grid assets rather than unregulated economic agents. Strategic investments in advanced load management and smart grid technologies are essential to provide the flexibility needed to manage these new demand dynamics. By addressing these challenges proactively, China can ensure its energy system remains robust and efficient, capable of supporting the next generation of technological innovation while achieving its ambitious environmental and economic goals.

While our study has provided insights into the adoption and impact of UFCS and ESS on urban power grids, it is based on certain core assumptions that shape the scope and applicability of our findings. For instance, our analysis assumes that technological and policy conditions, apart from those related to UFCS and TOU pricing, remain stable, which may not fully capture the dynamic nature of real-world energy markets and technological evolution. Additionally, our reliance on historical consumption patterns to predict future behaviors might not accurately reflect the rapidly changing consumer preferences and regulatory environments. Moreover, our assessment of grid risks primarily utilized the macro indicators, which might not capture the detailed behaviors and localized responses within microgrids. Subsequent research would benefit from integrating our demand-side findings with comprehensive power system models to assess system-wide stability impacts more accurately[52,53]. Incorporating dynamic models that adapt to technological advancements and policy shifts, along with richer datasets covering diverse economic conditions and granular consumer behavior, could also enhance future analyses[54]. These enhancements will allow for a more nuanced understanding of the complex interactions within urban energy systems and help refine strategies for integrating UFCS and ESS into increasingly diverse and volatile urban environments. This progression of research will be key to developing adaptable and resilient energy frameworks that can meet the needs of future urban landscapes.

Methods

Datasets

This study integrates multi-source datasets, including charging records, electricity pricing, EV ownership statistics, aggregated EV charging load, and urban power load profiles, for Beijing, Shanghai, and Guangzhou in China. Charging record data were collected from public stations in the three cities, comprising a dataset of 769,225 charging orders from 1,702 public charging stations and covering a 31 day period from January 18 to February 17, 2024. Each record provides detailed information on the location of the charging station, the specific charging gun used, the start and end times of the charging session, and the charging power (kW). The total charging load data and EV ownership statistics for Shanghai in 2023 were sourced from the State Grid Corporation of China[55]. Using this data as a reference, we estimated the total EV electricity consumption in Guangzhou and Beijing by extrapolating from the city's total EV ownership figures[56]. The urban power load profile data is provided by the National Development and Reform Commission[57].

Charging load estimation from charging order records

This study estimates the aggregated charging power demand in an urban area using public charging order data. Each record provides the start time, end time, and the rated power (P_r) of the charging station used. Recognizing that EV charging power is not constant, particularly during ultra-fast charging (UFC), which follows a characteristic Constant Current - Constant Voltage (CC-CV) profile[58], we employ a three-stage piecewise charging profile model for each individual charging session, which is denoted as:

$$P(t) = \begin{cases} P_r \frac{\tau}{\alpha}, & 0 \leq \tau \leq \alpha \\ P_r, & \alpha < \tau \leq \alpha + \beta \\ P_r - (P_r - P_{\text{end}})\frac{\tau - \alpha - \beta}{1 - \alpha - \beta}, & \alpha + \beta < \tau \leq 1 \end{cases} \quad (1)$$

Here t denotes the elapsed time, T the total session length, and $\tau = t/T$ the normalised time variable. This model incorporates 3 phases: (1) an initial linear ramp-up phase of duration αT (with $\alpha = 0.05$), (2) a constant-power plateau of duration βT at the charger's rated power P_r (with $\beta = 0.10$), and (3) a linear tail-off that mimics the constant-voltage stage in which the power tapers down to P_{end}. The parameters α and β are informed by typical high-power charging profiles reported in the literature[59].

The tail-power at the end of the CV taper P_{end} is denoted as:

$$P_{\text{end}} = 2\left[\bar{r} - \left(\frac{\alpha}{2} + \beta\right)\right]\frac{P_r}{1 - \alpha - \beta} - P_r \quad (2)$$

To ensure energy conservation, P_{end} is solved analytically so that the mean power coefficient $\bar{r} = \frac{1}{T}\int_0^T P(t)\,dt/P_r$ attains the empirically observed value $\bar{r} = 0.55$; this aligns with large-scale public-charging analyses, which show that the session-average power is usually 30–60% of P_r[60,61]. A lower bound of $0.1P_r$ is imposed on P_{end} to preclude unrealistically steep power drops.

After estimating the power load for each charging session, the total charging power at any given time t can be calculated as the sum of the power of all ongoing charging orders. The total charging load P_t is estimated as:

$$P_t = r\sum_i P_{i,t} \quad (3)$$

where $P_{i,t}$ represents the power of the i-th charging order active at time t, and r is a scaling factor introduced to account for the partial coverage of the charging station data.

Since the charging station order data used in this study represents a sample of the entire population of public charging stations within each city, the scaling factor r is applied to adjust the results accordingly, computed as:

$$r = \frac{EC_{\text{truth}}}{EC_{\text{order}}} \quad (4)$$

where EC_{truth} is the total annual charging energy consumption for EVs within the city, derived from official statistics or authoritative sources, and EC_{order} is the total annual charging energy consumption estimated from the charging order data. Using the methodology described, the overall charging power scale for the city can be estimated for any given time[62].

Categorization for charging stations

To accurately differentiate the functional roles of charging stations within complex urban environments, we employed a classification method based on station names and addresses processed by a Large Language Model (LLM), specifically OpenAI's GPT-4o-mini. Traditional methods often rely on geographic coordinates and land-use data and face challenges with the ambiguity in dense, mixed-use developments, where stations serving different purposes may be co-located. Station names and addresses provide richer contextual information regarding the operating entity, specific location within a facility, and intended clientele. Leveraging an LLM allows for a nuanced interpretation of this textual data, aiming for a more functionally accurate and consistent classification compared to solely coordinate-based approaches.

By providing station names and addresses as input, we utilized a tailored prompt designed to categorize each station as 'Residential', 'Commercial', 'Workplace', or 'Other' based on its operational characteristics. The prompt for categorization was constructed to guide the model in considering contextual clues from the station's name and address; it provides detailed guidelines on typical associations between certain types of locations and corresponding categorizations. In Guangzhou, the 410 EV charging stations are classified as 98 commercial stations, 152 workplace stations, 80 residential stations, and 80 other stations. In Shanghai, the 606 stations are classified as 243 commercial stations, 167 workplace stations, 171 residential stations, and 26 other stations. And in Beijing, the 686 stations are classified as 214 commercial stations, 255 workplace stations, 141 residential stations, and 76 other stations.

The prompt used and examples of the categorization results are provided in the Supplementary Note 3. This detailed categorization informed the simulation of UFCS deployment, where stations classified as Commercial and Workplace were prioritized for conversion to UFCS in the 2030 and 2035 scenarios to reflect likely initial rollout targeting high-traffic public and semi-public locations.

Simulation of charging load for UFCS

To investigate the grid-level impact of large-scale UFCS deployment, this study conducts a simulation based on real charging order data. The protocol is designed to strictly isolate the effects of increased charging power by systematically modifying a subset of existing charging records, ensuring that the underlying behavioral patterns observed in the empirical data are preserved.

The simulation process for each deployment scenario begins by establishing an upgrade quota within our sample data. This quota represents the pro-rata power capacity increase required to mirror a city-wide deployment of n UFCS stations. Specifically, we define the sample-level power addition quota, ΔP_{quota}, as:

$$\Delta P_{\text{quota}} = \frac{n \cdot k \cdot P_u}{r} \quad (5)$$

where n is the target number of UFCS to be deployed in the city, k is the number of ultra-fast charging guns per station, P_u is the rated power of a single UFCS gun, and r is the city-specific scaling factor defined in equation (4).

With this quota established, chargers within the sample are selected for an upgrade. Priority is given to those in 'Commercial' and 'Workplace' locations. A randomized selection process then iteratively designates individual chargers for upgrade until the cumulative sum of their power capacity increases meets or exceeds the quota ΔP_{quota}.

For each charging record associated with a charger designated for an upgrade, the simulation modifies the session's characteristics while holding its core attributes constant. Specifically, the empirically observed charging initiation time t_s and the total energy consumption E of the original order are preserved. The total energy E for each charging order is estimated from the original data as:

$$E = \bar{r} \cdot P_o \cdot (t_e - t_s) \quad (6)$$

where $t_e - t_s$ is the charging duration in hours and $\bar{r}$ is the mean power coefficient. Here, P_o denotes the rated power of the original, non-UFCS charger used for that session.

When upgrading standard charging stations to UFCS, it is assumed that the charging demand remains constant. Specifically, the energy E and the start time t_s of each order are unchanged, while the charging power is adjusted to the rated power of UFCS, denoted as P_u.

After transitioning to UFCS, the new end time t'_e for each order can be estimated based on the original energy E and the ultra-fast charging power P_u:

$$t'_e = t_s + \frac{E}{\bar{r} \cdot P_u} \quad (7)$$

Since $P_u > P_o$, the new end time t'_e will be shorter than the original end time t_e, reflecting the reduction in charging duration enabled by UFCS.

Risk assessment for exceeding regulating reserve

The deployment of UFCS can introduce significant load volatility at different times of the day[63]. To assess the potential stress on grid flexibility, we evaluate the risk of the charging-induced load changes exceeding the system's RR capacity. The RR represents the flexible

resources available to the system operator to manage short-term fluctuations in supply and demand. Exceeding this capacity implies that the rate of change in charging demand surpasses the system's ability to respond quickly, potentially jeopardizing grid stability.

First, we define the instantaneous ramping load, $R(t)$, introduced by UFCS at each time step t as the absolute difference between the load profile with UFCS and the original baseline load profile:

$$R(t) = |P_{base}(t) - P_{ufcs}(t)| \qquad (8)$$

where $P_{base}(t)$ is the baseline load at time t without UFCS deployment, and $P_{ufcs}(t)$ is the total load at time t including the simulated UFCS deployment.

Since the ramping load $R(t)$ can exhibit time-varying statistical properties, we employ a non-parametric approach using a sliding window and Kernel Density Estimation (KDE). For each time step t, we consider a window containing the ramping load values $R(\tau)$ for τ within a defined interval around t (e.g., $t \pm 30$ min, considering wrap-around at midnight). Let this set of windowed ramping loads be $\mathcal{R}_t$. We then apply KDE to the data in $\mathcal{R}_t$ to obtain a local estimate of the probability density function (PDF) of the ramping load at time t, denoted as $\hat{f}_t(r)$.

Given a specific threshold, the probability of exceeding this threshold at time t for a single UFCS deployment scenario is estimated by integrating the KDE-derived PDF:

$$P_{exceed}(t, \mathrm{RR}) = \int_{\mathrm{RR}}^{\infty} \hat{f}_t(r) dr \qquad (9)$$

Recognizing that the simulation of UFCS deployment involves random station selection, a single simulation might not capture the expected risk profile. Therefore, we perform $M = 50$ independent simulations for each UFCS deployment scenario. For each simulation, we calculate the corresponding UFCS load profile $P_{ufcs}^{(m)}(t)$ and the resulting time-series of probabilities $P_{exceed}^{(m)}(t, \mathrm{RR})$.

The final reported risk of exceeding the RR at time t for a given RR threshold is the average probability across all M simulations:

$$\bar{P}_{exceed}(t, \mathrm{RR}) = \frac{1}{M} \sum_{m=1}^{M} P_{exceed}^{(m)}(t, \mathrm{RR}) \qquad (10)$$

By varying the RR threshold and potentially the scale of UFCS deployment, we can derive comprehensive risk probability curves ($\bar{P}_{exceed}(t, \mathrm{RR})$ as a function of t and RR). These results provide quantitative insights into how UFCS deployment impacts the demands on system flexibility, highlighting critical time periods and reserve levels needed to maintain grid stability.

Risk assessment for exceeding capacity reserve

This analysis evaluates the risk that the total charging demand, amplified by large-scale UFCS deployment, exceeds the allocated CR. The CR represents the planned headroom above the typical peak load, designed to accommodate fluctuations and ensure system adequacy. We define the CR threshold, L_c, based on the historical peak load of the baseline charging demand ($P_{base, max}$) plus a predefined buffer percentage, c:

$$L_c = P_{base, max} \times (1 + c) \qquad (11)$$

where c represents the reserve margin (e.g., 15%, 20%, 25%). Exceeding this threshold indicates a potential strain on the planned grid resources allocated for EV charging.

To assess this risk probabilistically, bootstrap resampling was employed to robustly estimate the exceedance probability and its uncertainty given the limited sample size from Monte Carlo

simulations[64]. For a given UFCS deployment scenario, the following steps are performed:

Initially, we conduct M independent Monte Carlo simulations (e.g., $M = 50$) of the daily charging activity, incorporating the impact of the deployed UFCS. Each simulation i yields a full-day, minute-by-minute load profile $P_{ufcs}^{(i)}(t)$. From each profile, we extract the maximum load value, representing the simulated daily peak load for that run:

$$P_{peak}^{(i)} = \max_{t \in \mathrm{Day}} P_{ufcs}^{(i)}(t), \quad i = 1, 2, \ldots, M \qquad (12)$$

This process generates an initial sample of M peak load values, $\mathcal{P}_{peak} = \{P_{peak}^{(1)}, P_{peak}^{(2)}, \ldots, P_{peak}^{(M)}\}$, which reflects the potential variability of the daily peak under the given scenario.

To estimate the probability of exceeding the capacity threshold L_c and quantify the uncertainty arising from the finite initial sample size M, we utilize the Bootstrap method. We perform $B = 1000$ resampling iterations; in each iteration $b = 1, \ldots, B$, a bootstrap sample $\mathcal{P}_{peak}^{*b}$ is created by drawing M values with replacement from the initial peak load sample $\mathcal{P}_{peak}$. A Kernel Density Estimator (KDE) is fitted to the bootstrap sample $\mathcal{P}_{peak}^{*b}$, yielding an estimated probability density function (PDF) $\hat{f}^{*b}(p)$. The probability of exceeding the threshold L_c for this specific bootstrap iteration is calculated by integrating the KDE:

$$Prob^{*b}(L_c) = \int_{L_c}^{\infty} \hat{f}^{*b}(p) dp \qquad (13)$$

After completing B bootstrap iterations, we obtain a distribution of B probability estimates $\{Prob^{*1}(L_c), \ldots, Prob^{*B}(L_c)\}$. The final estimate for the probability of exceeding the CR L_c is the mean of these bootstrap estimates:

$$\bar{P}_{exceed}(L_c) = \frac{1}{B} \sum_{b=1}^{B} Prob^{*b}(L_c) \qquad (14)$$

The standard deviation of these B estimates, $S_{exceed}(L_c)$, provides a measure of the uncertainty associated with $\bar{P}_{exceed}(L_c)$, which can be visualized using error bars.

By systematically increasing the deployment scale of UFCS and calculating $\bar{P}_{exceed}(L_c)$ and $S_{exceed}(L_c)$ for different CR thresholds ($c = 15\%, 20\%, 25\%$), we generate risk probability curves. These results offer quantitative insights into how the penetration of UFCS influences the likelihood of challenging the grid's planned capacity margins, thereby identifying critical deployment levels and informing necessary grid reinforcement or demand management strategies.

Estimation of grid load for on-site integrated UFCS

To evaluate the impact of energy storage strategies at charging stations on the power grid, three scenarios were considered: unregulated market operation, capacity charge, and demand response control.

In the unregulated market scenario, charging and discharging strategies are driven solely by profit maximization (or cost minimization of energy procurement), allowing charging stations to replenish energy for storage without grid-imposed restrictions, focusing purely on arbitrage opportunities based on time-varying electricity prices.

The capacity charge scenario also aims to minimize cost but includes an additional charge based on the maximum power drawn from the grid over the optimization period. The corresponding fees are set to be 48 CNY/kW in Beijing, 40.8 CNY/kW in Shanghai, and 32 CNY/kW in Guangzhou in our model. This incentivizes stations to shave their peak load by using stored energy during high-demand moments and recharging during off-peak times. Each station

optimizes its operation considering both energy costs and its own peak demand cost.

Finally, the demand response control scenario introduces a hard control threshold L_{DR} (in kW or MW) for the total power drawn from the grid by all stations combined. Under this scenario, charging stations must ensure their aggregated energy replenishment stays below this threshold; if the cumulative charging demand would exceed the threshold, the replenishment is curtailed or deferred until overall grid conditions allow, ensuring grid stability.

To investigate the impact of UFCS with energy storage on the power grid in an unregulated market environment, revenue maximization is adopted as the optimization objective, reflecting the role of each charging station as an independent market participant[65–67]. In a competitive market, charging stations are economically motivated to optimize their charging and discharging strategies, aiming to maximize profitability while adapting to market dynamics. An optimization model is developed for each station to design energy storage strategies that align with this goal. The overall optimization framework is structured into two components: 1. Optimizing the total charging and discharging strategies for each pricing time period; 2. Distributing the optimized charging load across individual minutes within the respective periods.

In the first part, we establish a model to optimize the charging and discharging energy schedules for each price period at each charging station based on actual charging demand conditions. The objective focuses on minimizing the daily cost of electricity procurement while satisfying the constraints of the charging and discharging operations, considering energy losses[68]. The model divides the operation time into N periods, with each interval i having a duration Δt_i and a corresponding electricity price c_i.

The objective of the model is to minimize the daily cost of electricity procurement for the charging station equipped with an on-site ESS. The objective function is expressed as:

$$\min \sum_{i=1}^{N} c_i \cdot G_i \tag{15}$$

where G_i is the decision variable representing the total energy purchased from the grid by the charging station during period i.

This objective function represents the goal for the unregulated market and demand response scenarios. For the capacity charge scenario, the objective is expanded to include the cost associated with the peak power demand incurred by the station during the optimization horizon. Let c_{peak} be the capacity charge rate and $P_{peak,s}$ be a new decision variable representing the maximum power drawn from the grid by station s during any period within the horizon. The objective function for the capacity charge scenario becomes:

$$\min \sum_{i=1}^{N} c_i \cdot G_{i,s} + c_{peak} \cdot P_{peak,s} \tag{16}$$

where the index s denotes a specific charging station, and all variables ($G_{i,s}$, $Y_{d,i,s}$, $Y_{c,i,s}$, $SoC_{i,s}$) are implicitly defined per station. The variable $P_{peak,s} \geq 0$.

To incorporate the capacity charge, we introduce the peak power variable $P_{peak,s}$ mentioned above, and the following constraint linking the grid energy purchase $G_{i,s}$ in each period i to this peak power. The average power drawn from the grid during period i is $G_{i,s}/\Delta t_i$. The peak power variable $P_{peak,s}$ must be greater than or equal to the average power in any period:

$$G_{i,s} \leq P_{peak,s} \cdot \Delta t_i, \quad \forall i \in \{1, 2, \ldots, N\} \tag{17}$$

This constraint, combined with the minimization objective equation (16), ensures that $P_{peak,s}$ accurately reflects the highest period-average

power drawn from the grid, which is then penalized by the capacity charge c_{peak}. This constraint is only active in the capacity charge scenario.

The model includes the following constraints. Let $E_{ev,i}$ be the total EV charging energy demand in period i, obtained from prior simulations or historical data. We introduce two non-negative decision variables for the ESS energy exchange at the AC interface, with $Y_{d,i}$ representing the energy discharged from the ESS to the AC side during period i and $Y_{c,i}$ representing the energy charged into the ESS from the AC side during period i.

The AC-side energy balance for each period is:

$$G_i + Y_{d,i} = E_{ev,i} + Y_{c,i}, \quad \forall i \in \{1, 2, \ldots, N\} \tag{18}$$

with the non-negativity constraints:

$$G_i \geq 0, \quad Y_{d,i} \geq 0, \quad Y_{c,i} \geq 0, \quad \forall i \in \{1, 2, \ldots, N\} \tag{19}$$

The energy charged or discharged by the ESS during period i is limited by the system's AC power ratings and the period duration. Let $P_{ess,c}^{max}$ and $P_{ess,d}^{max}$ be the maximum AC charging and discharging power capacities of the ESS, respectively. The constraints are:

$$Y_{d,i} \leq P_{ess,d}^{max} \cdot \Delta t_i, \quad \forall i \in \{1, 2, \ldots, N\} \tag{20}$$

$$Y_{c,i} \leq P_{ess,c}^{max} \cdot \Delta t_i, \quad \forall i \in \{1, 2, \ldots, N\} \tag{21}$$

These limits ensure the energy transferred at the AC interface does not exceed the rated AC power during the period. Note that efficiency factors are not applied here as these variables represent AC-side energy.

To reflect periodic consistency, the storage system's state of charge (SoC) is required to be at the same level at the start and end of the optimization horizon:

$$SoC_N = SoC_0 \tag{22}$$

The initial SoC (SoC_0) is set based on operational assumptions. The SoC at the end of period i (SoC_i) evolves based on the SoC at the end of the previous period (SoC_{i-1}) and the energy charged or discharged in period i, explicitly considering charging (η_c) and discharging (η_d) efficiencies:

$$SoC_i = SoC_{i-1} - \frac{Y_{d,i}}{\eta_d} + (Y_{c,i} \cdot \eta_c), \quad \forall i \in \{1, 2, \ldots, N\} \tag{23}$$

This equation reflects that discharging $Y_{d,i}$ from the AC side requires drawing $Y_{d,i}/\eta_d$ from the internal storage, while charging $Y_{c,i}$ from the AC side only adds $Y_{c,i} \cdot \eta_c$ to the internal storage due to losses. The efficiencies η_c and η_d are derived from the AC-AC round-trip efficiency (η_{rt}), typically assuming $\eta_c = \eta_d = \sqrt{\eta_{rt}}$.

The SoC must remain within its operational limits throughout the process:

$$SoC_{\min} \leq SoC_i \leq SoC_{\max}, \quad \forall i \in \{1, 2, \ldots, N\} \tag{24}$$

where $SoC_{\min}$ and $SoC_{\max}$ represent the minimum and maximum allowable energy stored in the ESS.

Based on this model, we determine the optimal AC-side energy exchange schedule ($Y_{d,i,s}^*$ and $Y_{c,i,s}^*$) for each period i and station s. The net energy exchange for period i is $Y_{net,i,s}^* = Y_{d,i,s}^* - Y_{c,i,s}^*$. This schedule is then used in the second stage for minute-level power allocation. For the capacity charge scenario, the optimization also yields the optimal peak power target $P_{peak,s}^*$ for each station. This schedule

($Y^*_{net,i,s}$) and, if applicable, the peak target ($P^*_{peak,s}$), are then used in the second stage for minute-level power allocation.

The model is formulated as a linear program and solved using the OR-Tools library via Python. Detailed parameter settings for the ESS, including efficiency values, are presented in the Supplementary Note 6.

The second stage allocates the optimized period-level net energy target $Y^*_{net,i,s}$ into minute-level ESS power flows $p_{t,s}$ for each station s and minute t belonging to period i. $p_{t,s} < 0$ signifies charging (drawing power) and $p_{t,s} > 0$ signifies discharging (injecting power). The allocation logic depends on the chosen scenario and ensures that the cumulative energy transferred within each period i matches the target $Y^*_{net,i,s}$, while respecting operational constraints.

The allocated power $p_{t,s}$ for any ESS must instantaneously respect its physical power limits:

$$-C_{ch,s} \le p_{t,s} \le C_{dis,s} \qquad (25)$$

where $C_{ch,s}$ and $C_{dis,s}$ are the maximum charging and discharging power capacities of the ESS at station s, respectively.

The allocation of charging power ($p_{t,s} < 0$) is handled differently depending on the scenario:

For the unregulated market scenario, ESS charging requests are fulfilled up to the station's power limit $C_{ch,s}$ and the remaining energy target $|Y^*_{net,i,s}|$, without considering grid impact. Charging happens whenever $Y^*_{net,i,s} < 0$ dictates, regardless of grid load.

For the capacity charge scenario, the first-stage optimization determined an optimal peak power target $P^*_{peak,s}$ for each station s. During minute-level allocation, the ESS charging power $|p_{t,s}|$ is constrained such that the total power drawn by station s from the grid does not exceed its individual target $P^*_{peak,s}$. The grid power for station s at minute t is $G_{t,s} = d_{t,s} - p_{t,s}$, where $d_{t,s}$ is the EV charging demand at station s. When ESS charging is needed ($p_{t,s} < 0$), the allocation ensures $G_{t,s} \le P^*_{peak,s}$. If the desired charging $|p_{t,s}|_{desired}$ would violate this, $|p_{t,s}|$ is curtailed to $\max(0, P^*_{peak,s} - d_{t,s})$. This inherently encourages charging when the station's own load $d_{t,s}$ is low, thus respecting the optimized peak.

For the demand response control scenario, this mechanism uses a global threshold L_{DR} (in kW or MW) for the maximum allowable total power drawn from the grid by all stations. The total grid load at minute t is the sum of aggregated EV charging demand ($\sum_s d_{t,s}$) and the net ESS charging power ($\sum_{s,p_{t,s}<0} |p_{t,s}|$). When the anticipated total load (based on desired ESS charging) exceeds L_{DR}, a proportional scaling logic is activated. The simulation calculates the available grid capacity remaining below L_{DR} after accounting for EV demand and any ESS discharging ($p_{t,s} > 0$). This available capacity is then distributed proportionally among all stations requesting ESS charging power ($p_{t,s} < 0$) for that minute. Each station's allocated charging power $|p_{t,s}|$ is scaled down by a common factor, ensuring the total grid load remains at or below L_{DR} while fairly sharing the necessary curtailment.

Crucially, the sum of the allocated minute-level power flows must satisfy the optimized energy target for each period i from the previous stage:

$$\sum_{t \in i} p_{t,s} \approx Y^*_{net,i,s} \qquad (26)$$

The simulation iterates minute-by-minute, determining $p_{t,s}$ based on the required energy $y^*_{i,s}$, instantaneous constraints (equation (25)), and the demand response mechanism. A detailed algorithm implementing this distribution and demand response logic is provided in Supplementary Note 6.

Data availability

The primary data supporting the findings of this study, specifically the electric vehicle charging records from 1,702 public stations in Beijing, Shanghai, and Guangzhou, have been deposited in the figshare repository under the accession code https://doi.org/10.6084/m9.figshare.28263986.

Code availability

The code used for the analysis in this study is publicly available in the GitHub repository: https://github.com/ni1o1/UFCSsim and has been permanently archived on Zenodo with the https://doi.org/10.5281/zenodo.15867160. Analysis and figure generation were performed using Python.

References

1. United Nations Framework Convention on Climate Change. *ParisAagreement Adopted at the 21st Conference of The Parties (COP21), Paris,* https://unfccc.int (2015).
2. Shafiei, E. et al. Macroeconomic effects of fiscal incentives to promote electric vehicles in iceland: implications for government and consumer costs. *Energy Policy* **114**, 431–443 (2018).
3. Rietmann, N. & Lieven, T. A comparison of policy measures promoting electric vehicles in 20 countries. In *The Governance of Smart Transportation Systems,* (eds. Finger, M. Audouin, M.) 125–145 (Springer, 2019).
4. International Energy Agency. *Trends in Electric Vehicle Charging.* https://www.iea.org/reports/global-ev-outlook-2024/trends-in-electric-vehicle-charging (2024).
5. TE Connectivity Corporation. *The Future Of High-powered Ev Charging: The Technical Considerations For Ensuring Efficient, Reliable Vehicle Charging.* https://chargedevs.com/ (2022).
6. Hawkins, A. J. *Volvo And Polestar Evs Are Now Getting Tesla Supercharger Access.* https://www.theverge.com/2024/10/29/24282667/volvo-polestar-tesla-supercharger-adapter-nacs (2024).
7. International Energy Agency. *Trends in Charging Infrastructure.* https://www.iea.org/reports/global-ev-outlook-2023/trends-in-charging-infrastructure (2021).
8. Shenzhen Administration for Market Regulation. *Classification And Evaluation Specification For Supercharging Equipment Of Electric Vehicles.* https://amr.sz.gov.cn/xxgk/xwzx/mtbd/content/post_11206918.html (2024).
9. International Energy Agency. *Global Ev Outlook 2023.* https://www.iea.org/reports/global-ev-outlook-2023/trends-in-charging-infrastructure (2021).
10. Huawei Technologies Co., Ltd. China High-Voltage Fast Charging Industry Development Report (2023-2025) (2023).
11. General Office of the State Council, PRC. *New Energy Vehicle Industry Development Plan (2021-2035).* https://www.theicct.org (2020).
12. Shanghai Municipal People's Government. *Three-Year Action Plan for Beautiful Shanghai Construction (2024–2026).* https://www.shanghai.gov.cn/nw12344/20240430/bc21f158df87493a85e53d34441a40b5.html (2024).
13. California Public Utilities Commission. *Decision 15-07-001: Decision On Residential Rate Reform For Pacific Gas And Electric Company, Southern California Edison Company And San Diego Gas & Electric Company And Transition To Time-of-use Rates.* https://www.cpuc.ca.gov/industries-and-topics/electrical-energy/electric-rates (2015).
14. Ontario Energy Board. *Regulated Price Plan Price Report— Ultra-low Overnight Prices (May 1 2023–October 31 2023).*

https://www.oeb.ca/sites/default/files/rpp-price-report-ULO-20230411.pdf (2023).

15. Government of Spain. *Royal Decree 216/2014 of 28 March Establishing the Methodology for Calculating the Voluntary Price for the Small Consumer of Electricity and Its Contractual Regime.* https://www.boe.es/buscar/doc.php?id=BOE-A-2014-3376 (2014).

16. Muratori, M. Impact of uncoordinated plug-in electric vehicle charging on residential power demand. *Nat. Energy* **3**, 193–201 (2018).

17. Yang, Y., Yang, S., Moon, H. & Woo, J. Analyzing heterogeneous electric vehicle charging preferences for strategic time-of-use tariff design and infrastructure development: a latent class approach. *Appl. Energy* **374**, 124074 (2024).

18. Vuelvas, J., Ruiz, F. & Gruosso, G. A time-of-use pricing strategy for managing electric vehicle clusters. *Sustain. Energy Grids Netw.* **25**, 100411 (2021).

19. National Development and Reform Commission (PRC). *Notice On Further Improving The Time-of-use Tariff Mechanism (ndrc Price [2021] No. 1093).* https://www.ndrc.gov.cn/xxgk/zcfb/tz/202107/t20210729_1292067.html (2021).

20. Shanghai Municipal Government. *Notice On Further Improving The Time Of Use Electricity Pricing Mechanism In Our City.* https://www.shanghai.gov.cn/gwk/search/content/e2652e3ab7ee49438d6e82af8880b160 (2024).

21. Guangdong Provincial Development and Reform Commission. *Notice On Further Improving The Peak Valley Time Of Use Electricity Price Policy In Our Province.* http://drc.gd.gov.cn/ywtz/content/post_3500421.html (2024).

22. Liu, X. et al. Transforming public transport depots into profitable energy hubs. *Nat. Energy* **9**, 1206–1219 (2024).

23. Jones, C. B. et al. Impact of electric vehicle customer response to time-of-use rates on distribution power grids. *Energy Rep.* **8**, 8225–8235 (2022).

24. Muttaqi, K. M., Isac, E., Mandal, A., Sutanto, D. & Akter, S. Fast and random charging of electric vehicles and its impacts: State-of-the-art technologies and case studies. *Electr. Power Syst. Res.* **226**, 109899 (2024).

25. Powell, S., Cezar, G. V., Min, L., Azevedo, I. M. & Rajagopal, R. Charging infrastructure access and operation to reduce the grid impacts of deep electric vehicle adoption. *Nat. Energy* **7**, 932–945 (2022).

26. Iannuzzi, D. & Franzese, P. Ultrafast charging station for electrical vehicles: dynamic modelling, design and control strategy. *Math. Comp. Simul.* **184**, 225–243 (2021).

27. Yang, D., Sarma, N. J., Hyland, M. F. & Jayakrishnan, R. Dynamic modeling and real-time management of a system of ev fast-charging stations. *Transportation Res. C. Emerg. Technol.* **128**, 103186 (2021).

28. Mohammed, A., Saif, O., Abo-Adma, M., Fahmy, A. & Elazab, R. Strategies and sustainability in fast charging station deployment for electric vehicles. *Sci. Rep.,* **14**, 283 (2024).

29. Chen, X. et al. Impacts of fleet types and charging modes for electric vehicles on emissions under different penetrations of wind power. *Nat. Energy* **3**, 413–421 (2018).

30. Zhuang, P. & Liang, H. Stochastic energy management of electric bus charging stations with renewable energy integration and b2g capabilities. *IEEE Trans. Sustain. Energy* **12**, 1206–1216 (2020).

31. Amry, Y., Elbouchikhi, E., Le Gall, F., Ghogho, M. & El Hani, S. Optimal sizing and energy management strategy for ev workplace charging station considering pv and flywheel energy storage system. *J. Energy Storage* **62**, 106937 (2023).

32. Silva, C. A., Andrade, J. R., Bessa, R. J. & Lobo, F. Dynamic pricing in ev charging stations with renewable energy and battery storage. In *2024 20th International Conference on the European Energy Market (EEM),* 1–7 (IEEE, 2024).

33. Sarker, M. R., Pandžić, H., Sun, K. & Ortega-Vazquez, M. A. Optimal operation of aggregated electric vehicle charging stations coupled with energy storage. *IET Gener. Trans. Distrib.* **12**, 1127–1136 (2018).

34. Bagherzadeh, E., Ghiasian, A. & Rabiee, A. Long-term profit for electric vehicle charging stations: a stochastic optimization approach. *Sustain. Energy Grids Netw.* **24**, 100391 (2020).

35. Lu, Q. et al. Decarbonization scenarios and carbon reduction potential for china's road transportation by 2060. *NPJ Urban Sustain.* **2**, 34 (2022).

36. China Society of Automotive Engineers. *Research On The Development Strategy And Roadmap Of Electric Vehicle Charging Infrastructure In China (2021–2035).* https://www.efchina.org/Reports-en/report-ctp-20211015-en (2021).

37. Yu, Q. et al. Modeling electric vehicle behavior: Insights from long-term charging and energy consumption patterns through empirical trajectory data. *Appl. Energy* **380**, 125066 (2025).

38. North American Electric Reliability Corporation. *Bal-002-wecc-3: Contingency Reserve.* https://www.nerc.com/pa/Stand/Reliability%20Standards/BAL-002-WECC-3.pdf (2024).

39. National Development and Reform Commission of the People's Republic of China. *National Development and Reform Commission. Provisional Measures for Power Reliability Management* (in Chinese). (National Development and Reform Commission of the People's Republic of China, 2022).

40. National Development and Reform Commission of the People's Republic of China. *Interim Measures for Electricity Reliability Management.* https://zfxxgk.ndrc.gov.cn/upload/images/20227/20227511262348.pdf (2022).

41. Federal Energy Regulatory Commission. *Winter Reliability Assessment 2023–2024.* https://www.ferc.gov/sites/default/files/2023-11/24_Winter-Assessment_1116_1020.pdf (2023).

42. Tian, J., Wang, P. & Zhu, D. Overview of chinese new energy vehicle industry and policy development. *Green. Energy Resour.* **2**, 100075 (2024).

43. Bailey, M. R., Brown, D. P., Myers, E., Shaffer, B. C. & Wolak, F. A. *Electric Vehicles And The Energy Transition: Unintended Consequences Of A Common Retail Rate Design.* https://www.nber.org/papers/w32886 (2024).

44. Kundur, P. et al. Power system stability. *Power Syst. Stab. Control* **10**, 7–1 (2007).

45. Denholm, P., Mai, T., Kenyon, R. W., Kroposki, B. & O'Malley, M. *Inertia And The Power Grid: A Guide Without The Spin.* https://docs.nrel.gov/docs/fy20osti/73856.pdf (2020).

46. Yang, M., Zhang, L., Zhao, Z. & Wang, L. Comprehensive benefits analysis of electric vehicle charging station integrated photovoltaic and energy storage. *J. Clean. Prod.* **302**, 126967 (2021).

47. Khan, F. A. et al. Design and development of grid independent integrated energy system for electric vehicle charging stations at different locations in malaysia. *Energy* **302**, 131686 (2024).

48. Emmanuel, M., Doubleday, K., Cakir, B., Marković, M. & Hodge, B.-M. A review of power system planning and operational models for flexibility assessment in high solar energy penetration scenarios. *Sol. Energy* **210**, 169–180 (2020).

49. Li, J., Liu, F., Li, Z., Shao, C. & Liu, X. Grid-side flexibility of power systems in integrating large-scale renewable generations: a critical review on concepts, formulations and solution approaches. *Renew. Sustain. Energy Rev.* **93**, 272–284 (2018).

50. Khuntia, S. R., Rueda, J. L. & van Der Meijden, M. A. Forecasting the load of electrical power systems in mid-and long-term horizons: a review. *IET Gen. Trans. Distrib.* **10**, 3971–3977 (2016).

51. Kell, A. J., McGough, A. S. & Forshaw, M. The impact of online machine-learning methods on long-term investment decisions and generator utilization in electricity markets. *Sustain. Comput. Inform. Syst.* **30**, 100532 (2021).

52. Yao, M., Roy, S. & Mathieu, J. L. Using demand response to improve power system small-signal stability. *Sustain. Energy Grids Netw.* **36**, 101214 (2023).

53. Duan, C., Chakraborty, P., Nishikawa, T. & Motter, A. E. Hierarchical power flow control in smart grids: Enhancing rotor angle and frequency stability with demand-side flexibility. *IEEE Trans. Control Netw. Syst.* **8**, 1046–1058 (2021).

54. Zheng, X. et al. A multi-scale time-series dataset with benchmark for machine learning in decarbonized energy grids. *Sci. Data* **9**, 359 (2022).

55. Li, Y. *Shanghai's Electric Vehicle Charging Volume Increases By 90% Year-On-Year In 2023*. https://www.chinanews.com.cn/cj/2024/01-20/10149776.shtml (2024).

56. Guangzhou Transport Planning Research Institute Co., L. *The 2023 Guangzhou Transportation Development Annual Report*. http://www.guangzhou.gov.cn/202408/02/156098_54695531.htm (2024).

57. National Development and Reform Commission. *Notice Of The National Development And Reform Commission On Doing A Good Job In Signing Medium - And Long Term Electricity Contracts In 2020*. https://www.ndrc.gov.cn/xxgk/zcfb/tz/201912/t20191230_1216857_ext.html (2024).

58. Li, Y. et al. Optimized charging of lithium-ion battery for electric vehicles: adaptive multistage constant current–constant voltage charging strategy. *Renew. Energy* **146**, 2688–2699 (2020).

59. Dunckley, J. *Dcfc Load Factor: What Are We Seeing Out In The Wild?* https://www.akenergyauthority.org/Portals/0/Alaska%20Electric%20Vehicle%20Working%20Group/2021.12.07%20DCFC%20Load%20Factor%20Presentation%20by%20EPRI.pdf (2022).

60. Hecht, C., Figgener, J. & Sauer, D. U. Analysis of electric vehicle charging station usage and profitability in germany based on empirical data. *iScience* **25**, 105634 (2022).

61. EV Database. *EV Database*. https://ev-database.org/ (2025).

62. Brinkel, N., Schram, W., AlSkaif, T., Lampropoulos, I. & Van Sark, W. Should we reinforce the grid? cost and emission optimization of electric vehicle charging under different transformer limits. *Appl. Energy* **276**, 115285 (2020).

63. Kumar, D. S., Maharjan, S. & Srinivasan, D. et al. Ramp-rate limiting strategies to alleviate the impact of pv power ramping on voltage fluctuations using energy storage systems. *Sol. Energy* **234**, 377–386 (2022).

64. Dixon, P. M. *Bootstrap Resampling* (John Wiley & Sons, Ltd, 2006).

65. He, G., Chen, Q., Moutis, P., Kar, S. & Whitacre, J. F. An intertemporal decision framework for electrochemical energy storage management. *Nat. Energy* **3**, 404–412 (2018).

66. Das, K., Grapperon, A. L. T. P., Sørensen, P. E. & Hansen, A. D. Optimal battery operation for revenue maximization of wind-storage hybrid power plant. *Electr. Power Syst. Res.* **189**, 106631 (2020).

67. Lai, C. S. et al. Profit maximization for large-scale energy storage systems to enable fast ev charging infrastructure in distribution networks. *Energy* **259**, 124852 (2022).

68. Kwon, S., Ntaimo, L. & Gautam, N. Optimal day-ahead power procurement with renewable energy and demand response. *IEEE Trans. Power Syst.* **32**, 3924–3933 (2016).

69. Shanghai Municipal Commission of Commerce & Shanghai Municipal Informatization Center. *2023 Annual Monitoring Report on the Automotive Circulation Industry Information*. https://www.cpenet.com.cn/difang/202403/t20240304_1417591.html (2024).

70. Beijing Municipal Development and Reform Commission. *Report on the Implementation of Beijing's 2023 National Economic and Social Development Plan and the 2024 Draft Plan*. https://www.beijing.gov.cn/zhengce/zhengcefagui/202402/t20240201_3318505.html (2024).

71. Guangzhou Municipal Bureau of Planning and Natural Resources & Guangzhou Urban Planning & Design Survey Research Institute Co., Ltd. *2023 Annual Report on Guangzhou Transportation Development*. https://www.gz.gov.cn/zwgk/sjfb/sjkd/content/post_9339840.html (2024).

72. China Electric Vehicle Charging Infrastructure Promotion Alliance. *Annual Report on the Development of Electric Vehicle Charging Infrastructure in China (2023-2024)*. (China Electric Vehicle Charging Infrastructure Promotion Alliance, 2024).

73. Beijing Municipal Development and Reform Commission. *Notice on Further Improving the Time-of-Use Electricity Pricing Mechanism in Beijing*. https://fgw.beijing.gov.cn/zwgk/zcwj/bmwj/202308/t20230821_3202392.htm (2023).

74. Guangdong Provincial Development and Reform Commission. *Notice on Further Improving the Peak-Valley Time-of-Use Electricity Pricing Policy in Guangdong Province*. https://drc.gd.gov.cn/zwgk/ywxx/content/post_3497597.html (2021).

75. Shanghai Municipal Development and Reform Commission. *Notice on Further Improving the Time-of-Use Electricity Pricing Mechanism in Shanghai*. https://www.shanghai.gov.cn/nw12344/20221216/72d969c3b9f6497982c9a4a63746c5e3.html (2022).

Acknowledgements

Author contributions

P.Z., H.Z., and Q.Y. conceptualized the study. The methodology was developed by Q.Y., J.L., H.W., and H.Z. Q.Y. performed the data visualization and wrote the original draft. P.Z., J.Y., and H.Z. supervised the project. Q.Y., P.Z., J.L., H.W., J.Y., and H.Z. contributed to the revision, review, and editing of the final manuscript.

Competing interests

The authors declare no competing interests.

Additional information